THE ASTROPHYSICAL JOURNAL, 493:73–80, 1998 January 20


# THE COMPLEX CORE OF ABELL 2199: THE X-RAY AND RADIO INTERACTION

F. N. OWEN
National Radio Astronomy Observatory,[1] P.O. Box O, 1003 Lopezville Road, Socorro, NM 87801
AND
J. A. EILEK
Astrophysics Research Center, Department of Physics, New Mexico Institute of Mining and Technology, Socorro, NM 87801
*Received 1996 December 23; accepted 1997 June 24*

## ABSTRACT

The cluster Abell 2199 is one of the prototypical "cooling flow" clusters. Its central cD galaxy is host to a steep spectrum radio source of the type associated with cooling cores. In this paper, we combine radio data with new *ROSAT* HRI data to show that conditions in its inner core, $\lesssim 50$ kpc, are complex and interesting. Energy and momentum flux from the radio jet have been significant in the dynamics of the gas in the core. In addition, the Faraday data detects a dynamically important magnetic field there. The core of the X-ray luminous gas is not a simple, spherically symmetric cooling inflow. In addition, we believe the X-ray gas has had strong effects on the radio source. It seems to have disrupted the jet flow, which has led to a dynamical history very different from the usual radio galaxy. This particular source is much younger than the galaxy, which suggests the disruptive effects lead to an on-off duty cycle for such sources.

*Subject headings:* galaxies: clusters: individual (Abell 2199) — galaxies: elliptical and lenticular, cD — galaxies: jets — galaxies: magnetic fields — radio continuum: galaxies — X-rays: galaxies

## 1. INTRODUCTION

Cluster cores are interesting places. Many cluster centers have steep X-ray profiles and low X-ray temperatures, which have lead to models of spherically symmetric cooling flows (e.g., the review of Fabian 1994). It is becoming clear, however, that the central regions are more complex than this simple picture. There is evidence for transonic, turbulent flows (e.g., Baum 1992) and for dynamically important magnetic fields (Taylor, Barton, & Ge 1994; Eilek, Owen, & Wang 1997b), at least in the inner $\sim$10–50 kpc of strongly cooling cluster cores.

In addition, when the central galaxies in cooling cores host radio galaxies, these radio sources are not typical. They are more diffuse in appearance and have steeper radio spectra than most larger scale radio sources (e.g., Burns 1990; the halo of M87 is also a nearby example of this class [e.g., Feigelsen et al. 1987]). It seems very likely that these sources have a different dynamical history than the larger scale ones not generally found in cluster centers, and that their history has been affected by their position in the center of a dense cooling core.

In this paper, we combine X-ray and radio data to study the central dynamics of one such cooling core cluster, Abell 2199, with its embedded radio galaxy, 3C 338. This cluster seems quite normal dynamically, with no strong evidence of subclumps in the velocity data (Zabludoff, Huchra, & Geller 1990). It contains a central cD galaxy, NGC 6166. This galaxy appears to have a triple nucleus, which is likely to arise from a projection of very eccentric orbits (Lauer 1986) rather than from a tightly bound central system. The cluster redshift is $z = 0.0312$ (Hoessel, Gunn, & Thuan 1980), so that $1'$ corresponds to 36 kpc if $H_0 = 75$ km s$^{-1}$ Mpc$^{-1}$.

The X-ray distribution from this cluster is also quite regular, indeed rather dull, on large scales. The *Einstein* image (Forman & Jones 1982) shows smooth, roughly circular isophotes. Jones & Forman (1984) quote a core radius $\sim$210 kpc (converted to our $H_0 = 75$ km s$^{-1}$ Mpc$^{-1}$). The smooth distribution shows no particular signs of subclumping or merger activity. This cluster is one of the prototypical cooling cores: the inner regions show the characteristic X-ray excess relative to a King model fit. Arnaud (1985) finds a cooling radius $\sim$120 kpc, a central cooling time $\sim$0.8 Gyr, and a mass inflow $\sim 90\ M_\odot$ yr$^{-1}$. The more detailed cooling flow model of Thomas, Fabian, & Nulsen (1987) has similar numbers.

NGC 6166 contains a radio source, 3C 338. It is small (radial extent $\sim$35 kpc), has moderate power ($8.8 \times 10^{41}$ ergs s$^{-1}$ between 10 MHz and 100 GHz [data from Herbig & Readhead 1992] converted to $H_0 = 75$ km s$^{-1}$ Mpc$^{-1}$), a steep spectrum (the integrated spectrum is given in Herbig & Readhead, and the two-frequency spectral index distribution is given in Burns, Schwendeman, & White 1983), and is diffuse in appearance. Thus, it fits well in the class of cooling core radio sources. Newer radio data have been obtained by Feretti et al. (1993), who present VLB images of a two-sided core jet, and by Ge & Owen (1994), who made new VLA images with polarization and Faraday rotation data.

In this paper, we combine new *ROSAT* data with existing radio data to explore the interesting dynamics of the core of A2199. We find direct evidence of the effect of the radio source on the central X-ray luminous gas. In this region, at least, we find that the X-ray gas cannot be described by a simple, spherical cooling flow model. We then compare this radio source with standard models for "normal" radio sources, and we conclude that this source is relatively young and has been disrupted by the surrounding gas. We suspect

[1] The National Radio Astronomy Observatory is operated by Associated Universities, Inc., under contract with the National Science Foundation.

that this scenario may be typical of the class of cluster-center radio sources.

## 2. DATA: CENTRAL REGIONS OF A2199

The intracluster medium in Abell 2199 is smoothly distributed on large scales and appears to be sitting quietly in the potential well of the central galaxy. In Figure 1, we show an optical image of the central $\sim 4'$ of the cluster (the data were taken by Owen & White 1991). The elongation of the low surface brightness halo of NGC 6166 is apparent. Lauer (1986) finds the position angle of the optical isophotes $\sim 30°$, for the inner $\sim 30''$; Owen & White find the same position angle for the 24.5 mag arcsec$^{-2}$ isophote, on a scale of $\sim 100''$, $\sim 60$ kpc. As we shall show, the large-scale X-rays are consistent with this.

We obtained *ROSAT* HRI data of the inner $\sim 1000''$ ($\sim 600$ kpc) of the cluster. A total of 47,522 s of useful integration time was accumulated by the satellite in 1994 on Abell 2199. The observations were made during two time periods, 1994 February 3–5 and 1994 August 31–September 6, each with about half the total integration time. The $17'$ area we studied has 166,725 detected photons. Using $2''$ pixels, the peak on the image (at the nucleus of NGC 6166) had 27 photons. No identifications of discrete sources with optical objects were found on the combined image, except for the core of the central galaxy. Thus, no checks were possible on the default coordinate system. However, the positional agreement between the two parts of the integration is good, agreeing to within about $2''$ in each coordinate for the brighter discrete sources in the field, and so we have adopted the default coordinate system. The photon statistics are not good enough to attempt to track any pointing wander as in Morse (1994). However, the discrete sources within $6'$ of the nucleus in the final image are consistent with FWHMs of about $6''$ east-west and slightly less north-south. Since the peak on the image is not very large, features much larger than this are probably real. At the resolution we have used to display the X-ray emission, all the features described are seen on images made with either data set.

In Figure 2, we show a contour map of the field, smoothed to $56''$ resolution. We note that the isophotes remain smooth, with no particular evidence of substructure, and show only a modest ellipticity. We binned the unsmoothed data into circular rings to derive a luminosity

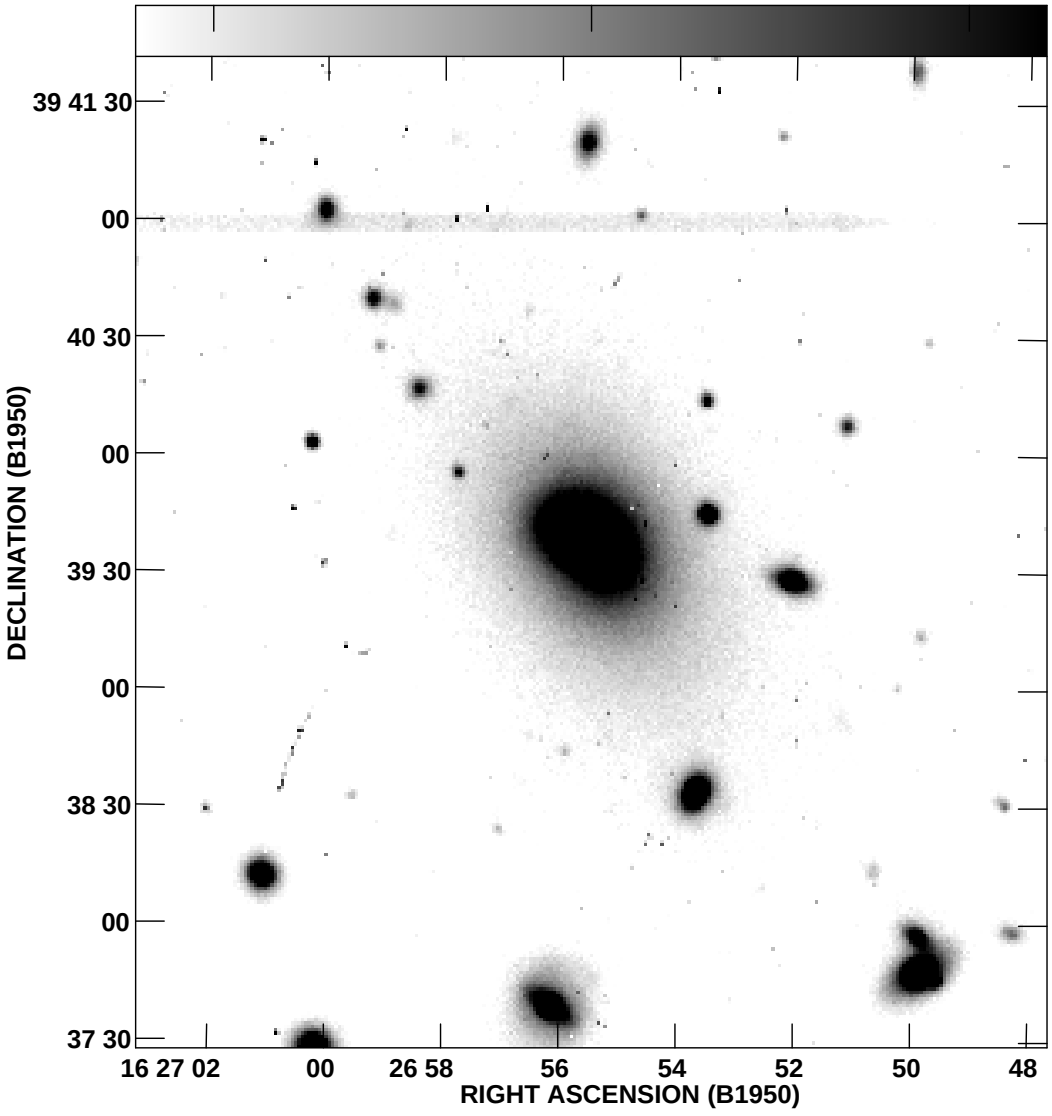


FIG. 1.—Optical image, obtained by Owen & White (1991), of the central region of the cluster Abell 2199. The cD galaxy NGC 6166 dominates the central region of the cluster.

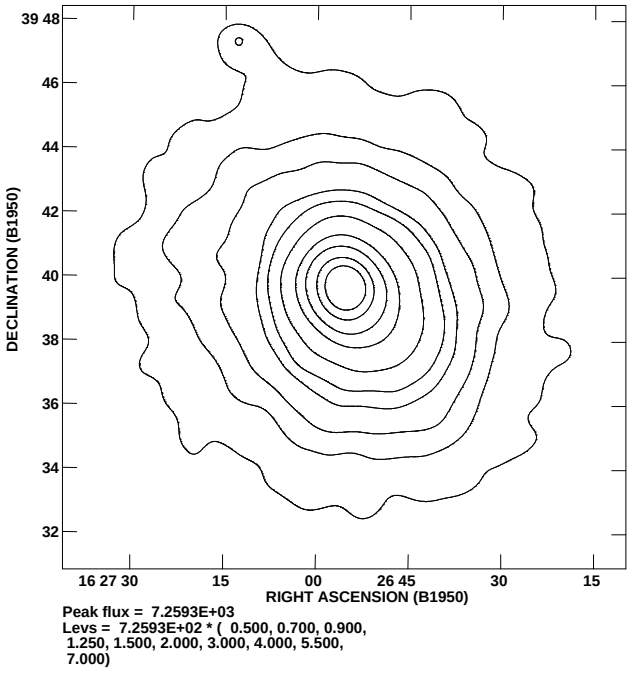


FIG. 2.—*ROSAT* HRI image of Abell 2199, smoothed to 56″ resolution. This choice gives a Gaussian beam of 1 arcmin$^2$. The units in this figure are counts per beam. Note the lack of substructure and the constancy of the isophote position angles on these scales.

profile, which is shown in Figure 3. The error bars in this figure assume Gaussian noise. From $\sim 1'$ to $\sim 10'$, the surface brightness follows a power law, $S_X(R) \propto R^{-1.2}$ if $R$ is the projected distance from the center. At smaller projected radii, our surface brightness profile continues to rise inward, but less rapidly. The *Einstein* data of Jones & Forman (1984) show a steeper falloff on larger scales, $S_X(R) \sim R^{-2.2}$

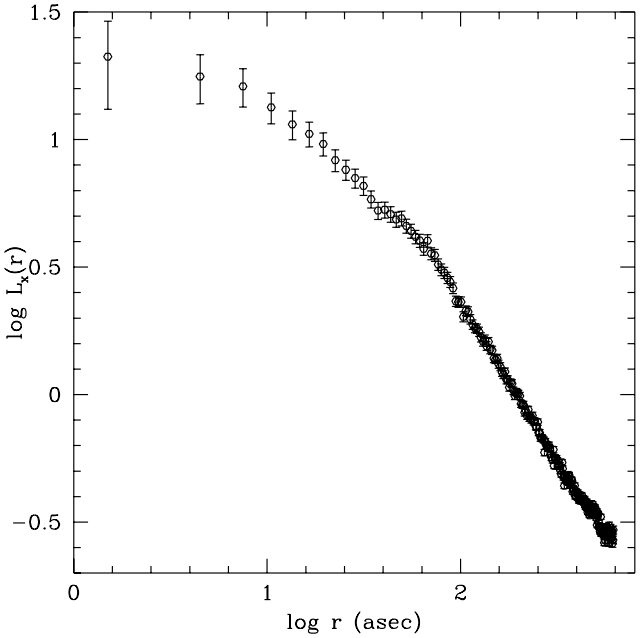


FIG. 3.—X-ray surface brightness of Abell 2199, obtained by binning the unsmoothed data into circular rings. The units of this figure are counts per pixel, where each image pixel is 2″ square. Note the shoulder at $r \sim 80''$, which is approximately the extent of the central radio source 3C 338.

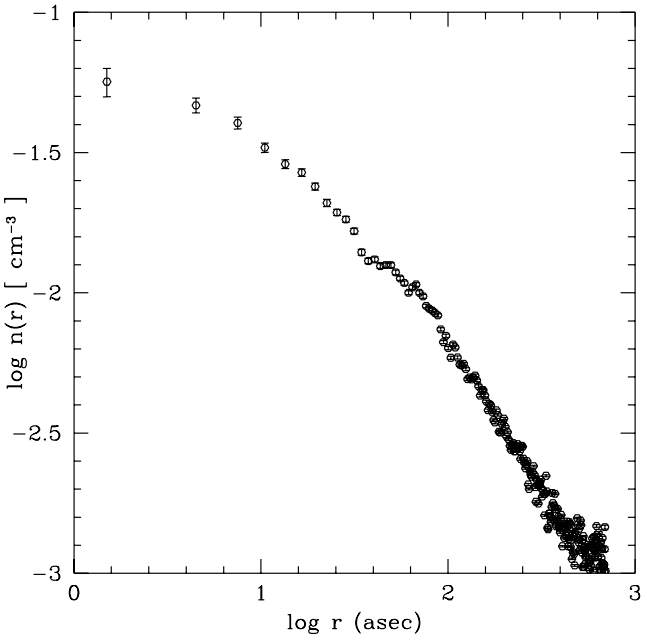


FIG. 4.—X-ray density of Abell 2199. We derived this by using an Abel transform on the data in Fig. 3 and by assuming a uniform temperature $T \simeq 2 \times 10^7$ K. Note the shoulder in the density distribution at $\sim 80''$.

for $R \gtrsim 5'$. Thus, a single power law is not a good fit to the entire cluster. We inverted the surface brightness with an Abel transform to find the radial emissivity profile of the cluster, out to $\sim 10'$.[2] To get the gas density, we assumed a temperature $T = 2 \times 10^7$ K (consistent with Thomas et al. 1987) throughout the cluster. (We note that the emissivity in the *ROSAT* band is not a sensitive function of the temperature, in this temperature range; this should provide a reliable measurement of the density.) We estimated the error in the de-projection by adding noise to each data point, chosen randomly in a $\pm\sigma$ range around the data; we repeated this random choice, and the Abel inversion, 100 times, and we determined the mean and standard deviation of the result. Our final density profile is shown in Figure 4. The gas density derived from this analysis also follows a good power law, $n_X(r) \propto n^{-1.2}$ past $r \sim 60$ kpc. Inside of this, it rises more gradually, as $n_X(r) \propto n^{-2/3}$, and approaches $n \sim 0.06\ \mathrm{cm}^{-3}$ as $r \to 0$.

In Figure 5, we show the ellipticities, and position angles, of elliptical isophotes fitted to the X-ray image using the IRAF program ELLIPSE. This program works its way from the solution at one radius to the next by considering a radius larger (or smaller) by a given fraction. In this case, the fraction used was 0.1. For this reason, the inner part of the profile is oversampled, and the errors are not independent. This does not affect any of the later analysis. On scales $\gtrsim 80''$ ($\sim 50$ kpc), the ellipticities and position angles remain approximately steady, at $\epsilon \sim 0.2$ and $\theta \sim 35°$, respectively. We note that the isophotes are not very elliptical, so that our spherically symmetric Abel inversion should be valid. In addition, in Figure 6 (Plate 4), we show an overlay of optical contours on the X-ray image, which demonstrates

[2] In order to reduce edge effects in the transform, we artificially extrapolated the measured $S_X(r)$, following the observed power law well past the last measured data point. This technique reduces the artificial turnup at large $r$ brought about by edge effects but, of course, adds an unsupported assumption to the large-scale structure we derive for scales $\gtrsim 200''$.

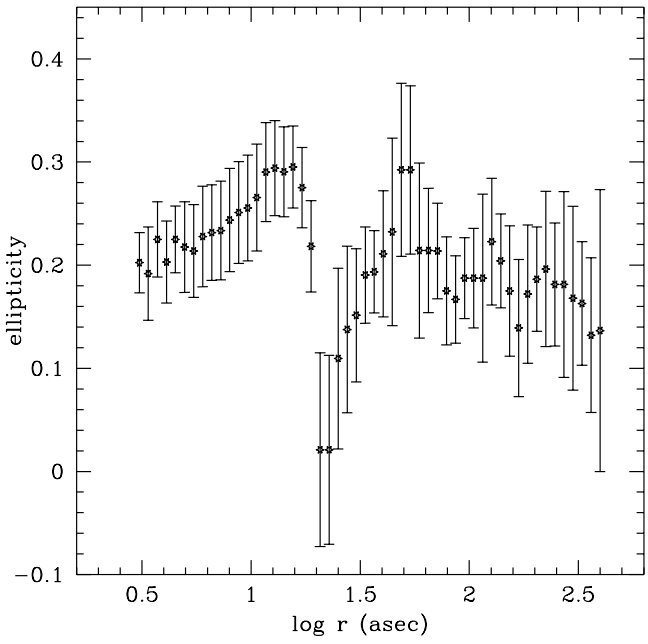


FIG. 5a

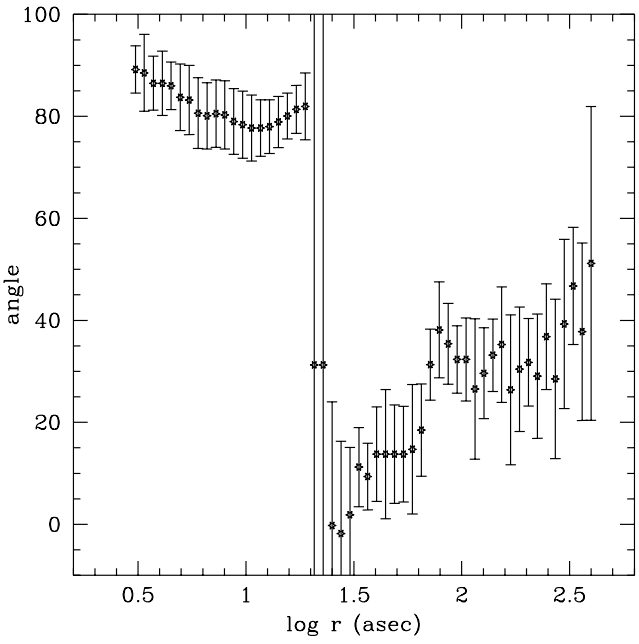


FIG. 5b

FIG. 5.—(*a*) Ellipticities of the X-ray isophotes. In this figure and the next, the profile is oversampled close to the nucleus, and therefore the errors in that region are not statistically independent. Note the increasing elongation from $r \sim 0''$ to $r \sim 16''$, the sudden drop there to nearly round isophotes, and the connection past that point to the large-scale $e \sim 0.2$ value. (*b*) Position angle of the isophotes. Note the dramatic difference between the inner isophotes, whose position angles are at right angles to the jet of the radio source, and the outer isophotes, whose position angles agree with the orientation of the cD galaxy.

that the position angle of the large-scale X-ray isophotes correlates well with the structure of the central galaxy.

Thus, the outer regions of the X-ray gas seem to be sitting quietly in the potential well of the galaxy. However, the region inside $\sim$50–60 kpc is more interesting. This is the region inside of which the X-ray isophotes (Fig. 5) change position angle and shape. For $r \lesssim 20''$, the isophotes have $\theta \sim 80°$; at this point, they rotate abruptly to $\theta \sim 15°$; past

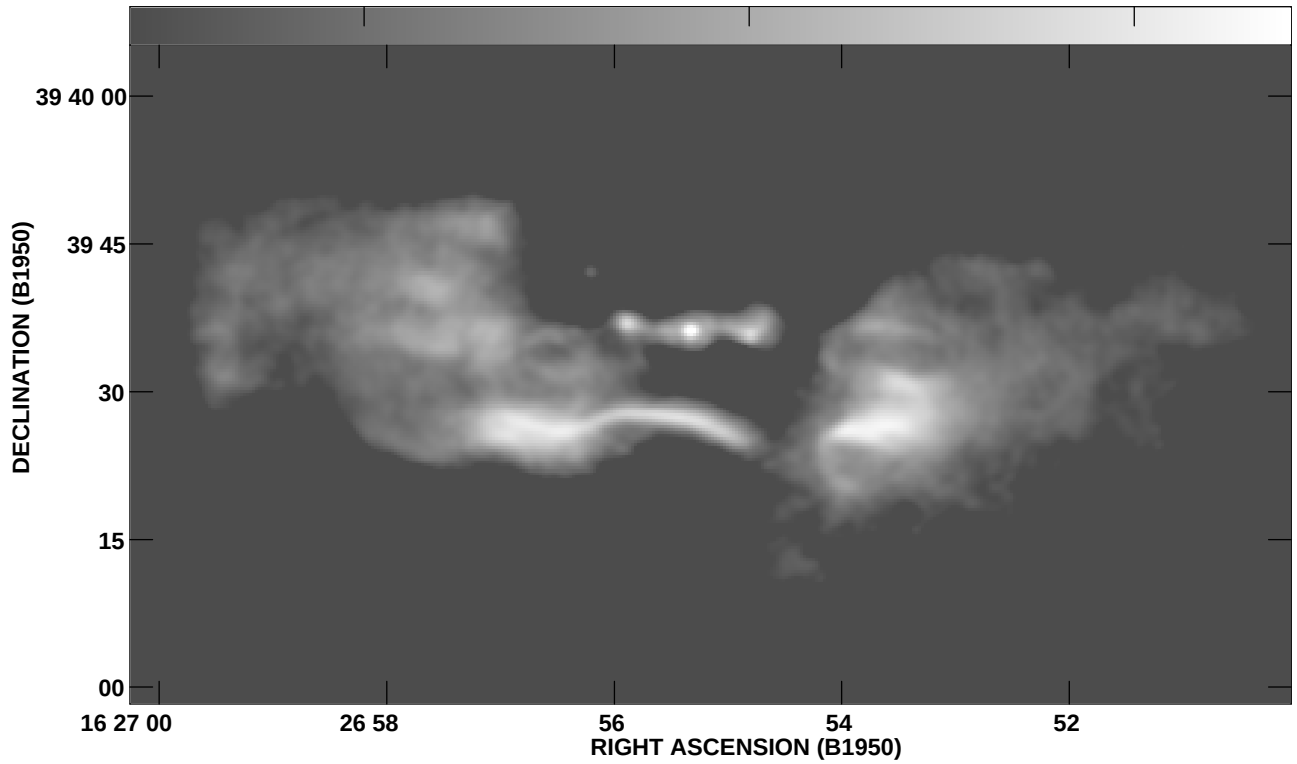


FIG. 7.—The 20 cm radio image of 3C 338 from Ge & Owen (1994). The radio core is in the center of the picture and is the source of short jets that terminate in the hot spots at $\pm$3 kpc to either side of the core. The gray-scale display is proportional to the tenth root of the intensity, in order to emphasize the fine structure and diffuse emission more clearly than is shown in Ge & Owen. The core coincides with the galactic nucleus and the VLB core and jet seen by Feretti et al. (1993). The bright filament to the south is not a jet; it seems to be simply a high-pressure shock or flux rope in the radio plasma.

here, they gradually rotate into alignment with the outer values. The ellipticity also changes; the very inner isophotes have $\epsilon \sim 0.2$–$0.3$; at $r \sim 20''$, they become round ($\epsilon \sim 0$); past this, they flatten slightly to agree, again, with the outer values.

In addition, the volume within $\sim 50''$ is that occupied by the radio source. In Figure 7, we show the 5 GHz image of 3C 338 from Ge & Owen (1994). The radio core coincides with the nucleus of NGC 6166 (Ge & Owen 1994), and also with the peak of the X-ray image using the coordinate system provided with the *ROSAT* database. A short jet, apparently ending in hot spots, is visible on either side of the core, extending $\sim 3$ kpc to a pair of hot spots. A two-sided nuclear jet has been detected on VLB scales (Feretti et al. 1993). The orientation of this jet coincides with the inner jet and hot spots on the VLA image. The bright ridge, or filament, south of the radio core does not coincide with any stellar feature; it is likely to be simply a high-emissivity filament, as is common in other sources (e.g., M87, Hines, Owen, & Eilek 1989; 3C 442, Comins & Owen 1991). The more diffuse radio lobes extend to $\sim 35$ kpc from its core, in our image and also in that of Burns et al. (1983). Roland, Hanisch, & Peltier (1990) searched but found no evidence for more extended, diffuse emission; the source seems to stop at $\sim 35$ kpc. We point out that the diffuse lobes also show nonuniform, filamentary internal structure.

The radio data also shows that the inner core contains magnetized thermal plasma (in addition to the magnetized relativistic plasma within the radio source). The Faraday rotation data of Ge & Owen (1994) show that rotation measures $\sim 1000$ rad m$^{-2}$, ordered on scales $\sim 3$ kpc, exist in the inner core. In the next section, we show that this is evidence of a dynamically important magnetic field in the core.

The complex dynamics of the inner core is also apparent in the central parts of the X-ray image. In Figures 8 and 9 (Plate 4), we show X-ray emission from the inner core, at higher resolution ($7''.5$), with the radio contours overlaid. From both figures, it is apparent that the radio source and X-ray luminous gas "know" about each other. Figure 8 shows that the inner X-ray gas extends almost directly to the north, for $\sim 40''$, at a right angle to the radio jet direction. Figure 9 shows that the very innermost X-ray gas is elongated east-west about $20''$, showing "ears" that coincide with the two radio hot spots at the ends of the inner jet.

Thus, the images suggest that the X-ray and radio sources are interacting on scales $\lesssim 50$ kpc in the inner core. In the next section, we explore this interaction.

## 3. DISCUSSION: DYNAMICS OF THE CENTER

The data show that the central regions of A2199 are not simple. The radio source and the X-ray luminous gas are interacting strongly. Existing "standard" models for each component (cooling flows for the X-ray gas, jet-driven dynamics for the radio source) must be modified to account for this interaction.

### 3.1. *Central Regions of Cluster Plasma*

The dynamics of the central $\sim 50$ kpc of A2199 are not well described by a spherically symmetric, cooling flow model. We find that the core contains a dynamically significant magnetic field, and that the radio source has a strong effect on the dynamics of the gas core.

The polarization data of Ge & Owen (1994) show that the core has a significant, ordered rotation measure (RM) distribution, and that the RM must come from foreground gas. In particular, the RM does not appear consistent with a totally random magnetic field; as with other sources (e.g., Taylor et al. 1994 or Eilek et al. 1997b), the sign and magnitude of the RM have a consistent, ordered pattern. We identify the foreground gas as the X-ray luminous gas in the cluster core. Taylor & Perley (1993) and Ge & Owen (1993) show that the rotation-producing gas in Hydra A and Abell 1975, respectively, is neither within the radio source nor from embedded emission-line clouds, nor in a mixing layer between the radio source and the cluster gas. Their arguments also apply to Abell 2199; thus, we take the X-ray–bright cluster gas to be the source of the rotation.

The data show that the RM has a typical magnitude $\sim 750$ rad m$^{-2}$; it has a typical order scale $\sim 3$ kpc. The depth of the RM patch along the line of sight is likely to be comparable, also $\sim 3$ kpc; since the source is larger than this, we are likely seeing "patches" or "flux ropes" of this scale in front of the source. If this typical RM comes from gas at density 0.02 cm$^{-3}$ (which we take as a typical value for the region from $\sim 4''$ to $\sim 80''$), the mean line-of-sight magnetic field is $\langle B_{\|} \rangle \sim 15$ $\mu$G. If we increase this by a $\sqrt{3}$ factor to account for likely projection, we estimate the mean magnetic pressure in the lobe region to be $\sim 2.8 \times 10^{-11}$ dyn cm$^{-2}$. For comparison, the pressure of the X-ray luminous gas in this region is $p_g = nkT \simeq 5.6 \times 10^{-11}$ dyn cm$^{-2}$ (for typical values in this core, we estimate $n \sim 0.02$ cm$^{-3}$ from our de-projection, and $T \sim 2 \times 10^7$ K as above). The typical magnetic pressure is thus significant compared with the ambient gas pressure.

The RM data also show one smaller, high-RM patch (a region with RM $\sim 1200$ rad m$^{-2}$, with scale $\sim 300$ pc) to the west of the nucleus (which can be seen in Fig. 3 of Ge & Owen 1994). If this is also the line-of-sight scale, this filament has $\langle B_{\|} \rangle \sim 250$ $\mu$G, and a minimum $p_B \sim 2.5 \times 10^{-9}$ dyn cm$^{-2}$. This is significantly higher than the ambient X-ray gas pressure. This suggests that the feature is strongly overpressured, and either locally self-confined magnetically or else transient. Of course, it is also possible that the RM of this filament is increased by local density fluctuations or a chance projection (with a longer line of sight, if we are looking along a long filament), or that the feature is somehow locally confined by its own field. Again, this says that the core plasma is magnetized, at a level that is important to its dynamics.

We also find that the gas distribution of the inner core has been affected by the radio source. As we pointed out above, inside of $\sim 50$ kpc, the distribution of the X-ray gas changes from the uniform ellipticity and position angle it shows on larger scales. In particular, the axes of the radio jets and of the inner X-ray isophotes are clearly connected (as in Figs. 8 and 9). These images suggest the following picture.

On the smallest scales, the radio jet is transferring momentum to the X-ray gas, pushing it out and causing the "ears" of X-ray emission around the jet. For instance, Chernin et al. (1994) modeled supersonic jets moving through a medium with a short cooling time. They find that high Mach number jets can transfer significant momentum to the ambient gas, *at the head of the jet*. Their calculation may be relevant here. Picking $n = 0.05$ cm$^{-3}$ for the inner few kiloparsecs, $T = 2 \times 10^7$ K, and using the Raymond,

Cox, & Smith (1976) emissivities give a cooling time $\sim 130$ Myr. This is only a few times larger that the dynamical age of the source, which we argue in the next section is on the order of tens of Myr.

In addition, the X-ray isophotes are elongated to the immediate north of the jet, opposite the direction of the radio lobes. This suggests that power from the radio source has been deposited in the inner X-ray gas, causing this structure. Quantitative estimates of the energetics of the core seem consistent with this. Let us recall that $P_{\rm rad} \sim 8.8 \times 10^{41}$ ergs s$^{-1}$. The beam power is most likely much larger (e.g., Eilek & Shore 1989). If we guess $\sim 1\%$ as a typical efficiency, the beam power is $P_b \sim 10^{44}$ ergs s$^{-1}$. Much of this beam power will be deposited in the ambient gas, as well as in the radio lobes themselves. We first note that the bolometric luminosity from the X-ray gas, using the Raymond et al. (1976) emissivities, is $L_{\rm core} \sim 2.4 \times 10^{43}$ ergs s$^{-1}$. (We calculated this for the inner 35 kpc of the X-ray core, the size of the radio lobes.) This is very similar to the likely $P_b$ value. Thus, the beam power clearly has a strong effect on the local thermal balance of the X-ray gas.

We can also estimate the energy content of the inner 35 kpc of gas. Its thermal energy content is $U_{\rm x} = (3/2)p_{\rm x} \simeq 2.6 \times 10^{59}$ ergs; its gravitational potential energy will be similar. The radio beam deposits this much energy in a time $U_{\rm x}/P_b \simeq 81/P_{44}$ Myr. This again argues that the radio source has had a significant effect on the energetics of the inner core and could have heated the "northern extension" of the X-ray gas enough to move it upward in the local gravitational potential.

### 3.2. *Cluster-Center Radio Source*

The radio source 3C 338 is typical of steep spectrum cluster-center radio sources. We suggest that it has developed from a jet that has been severely disrupted by the conditions in the central cooling core of this cluster. It follows that this is a relatively young source, and that such cluster-center galaxies must have an "on-off" cycle of radio activity.

We begin our argument with the appearance of the source. It is more diffuse than standard type I or type II radio galaxies; it shows neither strong external hot spots nor a directed tail flow emanating from the core. It does contain an active VLB jet, which connects to the 3 kpc scale VLA inner jets but does not continue into the lobes. Its diffuse appearance suggests that it has grown more as a "bubble," driven by its internal energy, than as a standard source driven by directed jet flow. The lobes are not particularly uniform. They are inhomogeneous, breaking up into filaments as in Figure 7; there is one bright ridge to the south of the core. These lobes are located to one side of the central core (opposite to the X-ray extension).

We also point out that the radio plasma must be separate from the X-ray luminous gas. If the two plasmas were well mixed, the high rotation measure found by Ge & Owen (1994) would depolarize the source (for example, a rotation measure of 750 rad m$^{-2}$ gives a Faraday depth $\sim 1.8$ rad at 6 cm; this would easily depolarize the source). Thus, the radio plasma cannot be well mixed with the local X-ray gas. This argues against diffusion as the origin of this source, and supports our suggestion of a "separate bubble."

The pressure within the radio source is consistent with our picture. We calculated the minimum pressure for the bright filament to the south of the radio core, and also for the diffuse lobes. In doing the calculation, we took the high-frequency spectral index $\alpha = 1.7$ from Burns et al. (1983) but assumed the spectrum flattened to $\alpha = 1.0$ between $10^7$ and $10^9$ Hz. (This give a more conservative estimate for the minimum pressure.) We also assumed a uniformly filled source and equal energy densities in relativistic protons and electrons. We found $p_{\rm min} \simeq 1.2 \times 10^{-10}$ dyn cm$^{-2}$ for the bright filament (corresponding to $B_{{\rm min},p} \simeq 42$ $\mu$G) and $p_{\rm min} \simeq 4.8 \times 10^{-12}$ dyn cm$^{-2}$ for the diffuse regions (giving $B_{{\rm min},p} \simeq 8$ $\mu$G). Thus, the bright filament is overpressured relative to the X-ray background (let us recall that $p_{\rm x} \sim 5.6 \times 10^{-11}$ dyn cm$^{-2}$ is typical of the inner $\sim 40$ kpc), while the lobes have $p_{\rm min} < p_{\rm x}$. The latter condition is compatible with pressure balance, because the true pressure in the radio source can exceed $p_{\rm min}$ easily; this will occur either if the source is inhomogeneous (as it clearly is) or if it is not exactly at the minimum pressure condition (which is physically quite possible). We suspect that overall pressure balance is maintained, and that the bright filament to the south is a transient feature, currently overpressured, due for instance to strong turbulence in the region.

What, then, is the dynamical history of this source? We suspect that the nuclear jet became unstable and disrupted severely, at approximately its current position of $\sim 3$ kpc from the core. We are not aware of numerical simulations that specifically address this situation. Hardee et al. (1992) modeled jets propagating in atmospheric gradients. Loken et al. (1993) modeled jets propagating in a strong cooling inflow. Both found that jets with lower Mach number can be stalled out or suffer strong instabilities that dramatically slow their propagation. After the instability has developed, the material flowing through the jet fills a "lobe" or "bubble" that grows only slowly thereafter. This bubble has now reached the lobe size, $\sim 35$ kpc. While neither of these calculations address the conditions that we find in A2199—a magnetized, probably turbulent, ambient medium—we suspect similar evolution may occur in this case.

If we adopt this model, we can estimate the dynamical age of the radio source. One clue comes from the 3 kpc length of the jet. Following Scheuer (1974), we apply momentum flux balance at the end of the jet. This predicts that a jet of opening angle $\Omega$, beam power $P_b$, and speed $v_b$ propagates into an ambient medium of density $\rho_{\rm x}$ at a rate given by

$$D(t) \simeq \sqrt{2}\left(\frac{P_b}{\Omega v_b \rho_{\rm x}}\right)^{1/4} t^{1/2} , \qquad (1)$$

where $\Omega v_b$ relates the beam power to its momentum flux. Models of type II radio source (Eilek 1997a) suggest $\xi = 100\Omega v_b/c \sim 1$, and we use this scaling here as well. Taking $n_{\rm x} \simeq 0.02$ from our X-ray data, the jet length expression becomes

$$D(t) \simeq 0.84\left(\frac{P_{44}}{\xi}\right)^{1/4} t_{\rm Myr}^{1/2} \text{ kpc} \qquad (2)$$

for propagation into a uniform medium at the density of the central X-ray gas. This predicts that the jet reaches 3 kpc in $t_{\rm jet} \sim 17$ Myr if $P_{44}/\xi = 1$. We suspect that it reached this point in this time, then suffered strong instabilities and disruption; thereafter, mass and energy transport continued, but not as a collimated flow. Therefore, the source must be at least as old as this.

A second constraint on the age comes from the expansion of the lobes. We envision them growing because of the internal pressure of the plasma that has passed through the end of the (now stalled) jet. Following Eilek & Shore (1989), we describe the evolution of such a lobe that expands at an approximate pressure balance with its surroundings:

$$V(t) \simeq \frac{P_b}{p_x} t \ . \tag{3}$$

Taking the X-ray pressure, $p_x \simeq 5.6 \times 10^{-11}$ dyn cm$^{-2}$, with $V = 4\pi R^3/3$ (ignoring nonsphericity), gives an estimate of the linear scale of the lobe:

$$R(t) \simeq 7.8(P_{44}\, t_{\rm Myr})^{1/3} \text{ kpc} \ , \tag{4}$$

so that the lobes have reached their current 35 kpc size in $t_{\rm vol} \sim 90$ Myr if $P \simeq 10^{44}$ ergs s$^{-1}$. Our picture is self-consistent in that this time is longer than the time needed for the central jet to reach its current scale.

One caveat here is that these calculations assume propagation into a uniform external medium. In reality, the ambient X-ray gas has a strong density and pressure gradient, as is apparent from Figures 3 and 4. This will accelerate both the jet propagation and the lobe growth. We are not aware of any specific models of such propagation but expect such affects to reduce $t_{\rm jet}$ and $t_{\rm vol}$, say, by a factor of 2 or so. In addition, one might expect buoyancy to be important in the lobe growth. This is also not included; we can estimate its effect by arguing that buoyant velocities will be no larger than the local gravitational speed. Fisher, Illingworth, & Franx (1995) measure the velocity dispersion $\sigma \sim 270$ km s$^{-1}$ for NGC 6166; from this, we can estimate $t_{\rm buoy} \sim 35$ kpc/$\sqrt{3\sigma} \sim 60$ Myr. This is comparable to $t_{\rm vol}$, suggesting that buoyancy will also reduce the growth time by an order unity factor.

Another possible estimate of the source age is from spectral steepening. Burns et al. (1983) take 400 MHz as the turnover frequency. If this applies throughout the source, we derive synchrotron ages of $\sim 70$ Myr for the diffuse lobes (with $B_{{\rm min},p} \sim 8$ $\mu$G) and $\sim 6$ Myr for the bright filament (with $B_{{\rm min},p} \sim 42$ $\mu$G). The larger of these numbers appears to be consistent with our dynamical ages. We caution, however, that spectral steepening by itself is not a reliable estimate of source ages; Eilek (1997b) demonstrates this for type I sources, and Eilek, Melrose, & Walker (1997a) discuss an alternative interpretation of the spectrum. Thus, we regard the coincidence of this estimate with our dynamical ages as interesting but not definitive.

Thus, our dynamical picture suggests that the source is young; it has taken no more than several tens of Myr to reach its current size. This is significantly younger than the age of the parent system.

## 4. CONCLUSIONS

In this paper, we presented new X-ray data that shows evidence of a complex interaction between the two plasmas (relativistic radio bright and thermal X-ray bright) in the core of A2199. We draw two major conclusions from this.

First, the core of this prototypical "cooling flow" is a complex place. The magnetic energy density (and one suspects turbulent energy densities) is comparable to that of the thermal gas. The radio source is an important source of energy for the X-ray gas in the core. Thus, this is not a simple symmetric cooling flow, at least on these scales. Second, the radio source shows signs of being disrupted by the ambient gas. It remains unmixed with the X-ray gas but has a different dynamical history than most radio galaxies. We suspect that this is a clue to the unusual nature of steep spectrum, cluster-center radio sources.

It is worth noting that M87 is another, very similar example of this phenomenon. The large-scale radio halo of M87 (e.g., Feigelsen et al. 1987) has a similar diffuse appearance and similar linear scale. The inner radio source of M87 has a jet that clearly disrupts on a scale of a few kiloparsecs (e.g., Owen, Hardee, & Cornwell 1989). The total radio power of M87 is very close to that of 3C 338 (Herbig & Readhead 1992), although the minimum pressure in the diffuse radio lobes is lower for M87 (Feigelsen et al. 1987). The inner regions of the X-ray halo of M87 have a similar run of pressure (Nulsen & Böhringer 1995) and also show evidence of dynamical interaction with the radio galaxy (Böhringer et al. 1995). Finally, the nuclear gas—at least on the few kiloparsecs scale—is also strongly magnetized (Owen, Eilek, & Keel 1990). Thus, at least one other system seems very similar to the one we have studied here

Finally, we note that steep spectrum radio sources are common in cDs in cooling cores; Burns (1990) detected such sources in $\sim \frac{2}{3}$ of his sample. While most have not been studied in detail, we suspect that 3C 338 and M87 are typical members of this class. If this is the case, the central cD must be radioactive for most of its life. This can only be reconciled with the relatively young age we deduce for 3C 338 ($\sim$30–100 Myr) if the parent galaxy has frequent, short-lived radioactive periods. Perhaps the instabilities that we now see disrupting the jet eventually shut it off totally, and after a quiescent period the system restarts itself.

We thank Chris Loken for useful discussions on jet disruption, and Fang Zhou for his help with the data. J. E. was partially supported by NASA grant NAG 51848 and NSF grant AST 91-17029.

## REFERENCES

Arnaud, K. 1985, Ph.D. thesis, Cambridge Univ.
Baum, S. 1992, in Clusters and Superclusters of Galaxies, ed. A. C. Fabian (Dordrecht: Kluwer), 171
Bohringer, J., Nulsen, P. E. J., Braun, R., & Fabian, A. C. 1995, MNRAS, 274, L67
Burns, J. O. 1990, AJ, 99, 14
Burns, J. O., Schwendeman, E., & White, R. A. 1983, ApJ, 271, 575
Chernin, L., Masson, C., de Gouveia Dal Pino, E. M., & Benz, W. 1994, ApJ, 426, 204
Comins, N. F., & Owen, F. N. 1991, ApJ, 382, 108
Eilek, J. A. 1997a, in preparation
———. 1997b, ApJ, submitted
Eilek, J. A., Melrose, D. B., & Walker, M. A. W. 1997a, ApJ, 483, 282
Eilek, J. A., Owen, F. N., & Wang, Q. 1997b, in preparation
Eilek, J. A., & Shore, S. N. 1989, ApJ, 342, 187
Fabian, A. C. 1994, ARA&A, 32, 277
Feigelsen, E. D., Wood, P. A. D., Schreier, E. J., Harris, D. E., & Reid, M. H. 1987, ApJ, 312, 101
Feretti, L., Comoretti, G., Giovannini, G., Venturi, T., & Wehrle, A. E. 1993, ApJ, 408, 446
Fisher, D., Illingworth, G., & Franx, M. 1995, ApJ, 438, 539
Forman, W., & Jones, C. J. 1982, ARA&A, 20, 547
Ge, J.-P., & Owen, F. N. 1993, AJ, 105, 778
———. 1994, AJ, 108, 1523
Hardee, P. E., White, R. E., III, Norman, M. L., Cooper, M. A., & Clarke, D. A. 1992, ApJ, 387, 460
Herbig, G., & Readhead, A. 1992, ApJS, 81, 83
Hines, D. C., Owen, F. N., & Eilek, J. A. 1989, ApJ, 347, 713

Hoessel, J. G., Gunn, J. E., & Thuan, T. X. 1980, ApJ, 241, 486
Jones, C. J., & Forman, W. 1984, ApJ, 276, 38
Lauer, T. 1986, ApJ, 311, 34
Loken, C., Burns, J. O., Norman, M. L., & Clarke, D. A. 1993, ApJ, 417, 515
Morse, J. A. 1994, PASP, 106, 675
Nulsen, P. E. J., & Böhringer, H. 1995, MNRAS, 274, 1093
Owen, F. N., Eilek, J. A., & Keel, W. 1990, ApJ, 362, 449
Owen, F. N., Hardee, P. E., & Cornwell, T. J. 1989, ApJ, 340, 698
Owen, F. N., & White, R. 1991, MNRAS, 249, 164
Raymond, J. C., Cox, D. P., & Smith, B. W. 1976, ApJ, 204, 290
Roland, J., Hanisch, R. J., & Peltier, G. 1990, A&A, 231, 327
Scheuer, P. A. G. 1974, MNRAS, 166, 513
Taylor, G. B., Barton, E. J., & Ge, J.-P. 1994, AJ, 107, 1942
Taylor, G. B., & Perley, R. A. 1993, ApJ, 416, 554
Thomas, P. A., Fabian, A. C., & Nulsen, P. E. H. 1987, MNRAS, 228, 973
Zabludoff, A. I., Huchra, J. P., & Geller, M. J. 1990, ApJS, 74, 1

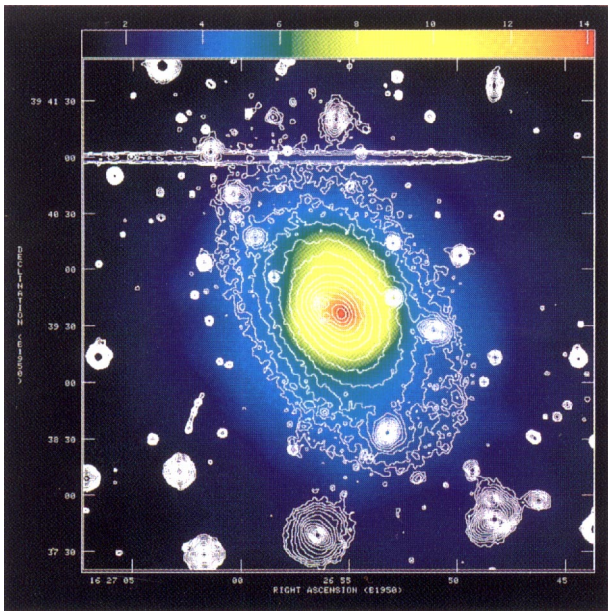

FIG. 6

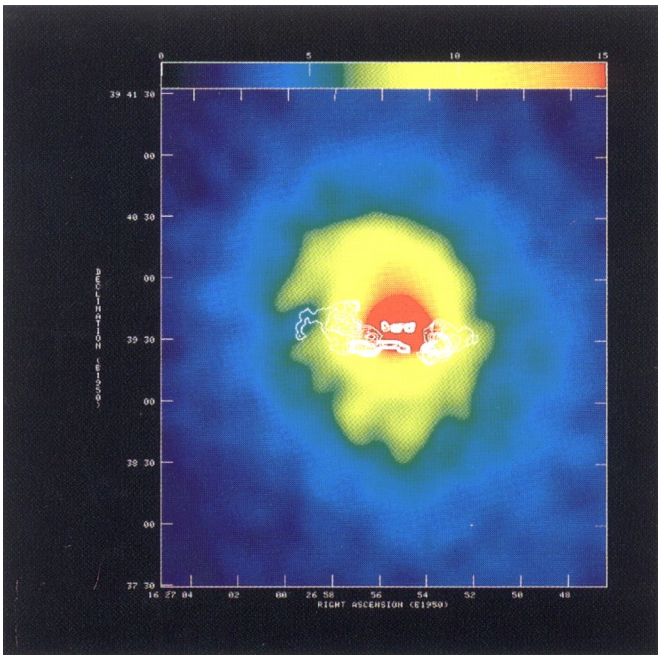

FIG. 8

FIG. 6.—Overlay of the optical image (*contours*) and the X-ray image (*color*), demonstrating the good agreement of the orientation of the stellar galaxy and the X-ray bright gas on these scales.
OWEN & EILEK (see 489, 75)

FIG. 8.—Overlay of the radio image (*contours*) and the X-ray image (*color*). This figure illustrates the $r \lesssim 35$ kpc scales on which the X-ray gas is elongated north-south and seems to be strongly affected by the radio source.
OWEN & EILEK (see 489, 77)

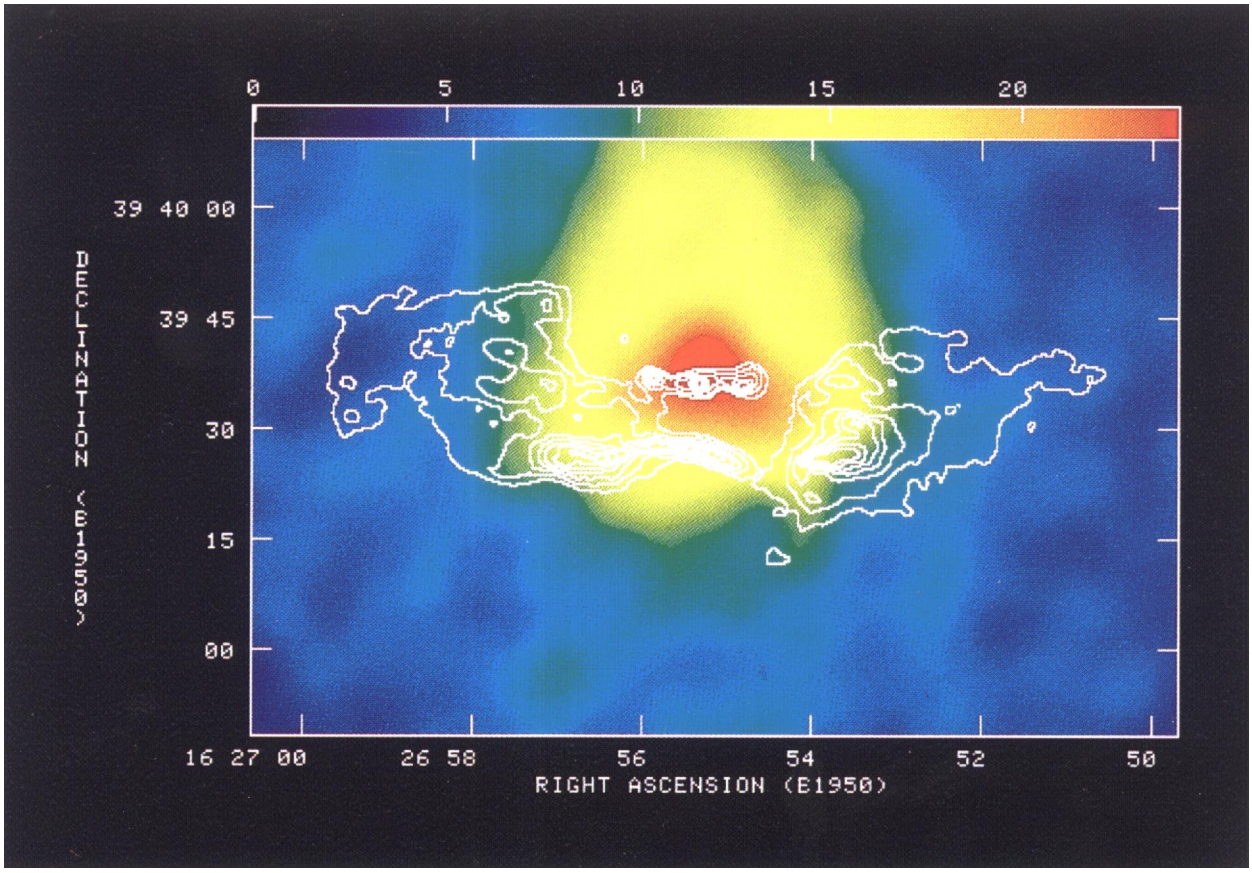


FIG. 9.—Overlay of the radio and X-ray images that is similar to Fig. 8, but illustrating the smallest scales ($\lesssim 5$ kpc, seen as the orange-red central region) on which the X-ray gas is elongated east-west and seems to be receiving momentum transferred from the radio jet.
OWEN & EILEK (see 489, 77)

PLATE 4